FRAME ASSEMBLY TESTS TO VERIFY THE EFFCTS OF FLOOR SLABS ON THE FLEXURAL BEAM STRENGTH

Toshimi Kabeyasawa[1], Toshikazu Kabeyasawa[2]

[1] *Professor Emeritus, The University of Tokyo, kabe@eri.u-tokyo.ac.jp*
[2] *Associate Professor, Tokyo Metropolitan University, tosikazu0911@gmail.com*

Abstract

A series of experimental and analytical investigations were conducted from 2010 to 2018 in order to verify the effects of floor slabs on the flexural strength of beams in reinforced concrete buildings against seismic loadings. The effective widths adopted in the current codes of practice were further validated for more accurate evaluation of lateral loading carrying capacity as well as for ensuring the beam-yielding mechanism of moment-resisting frame structures. A total of seven frame assemblies were tested: two in 2010, three in 2013, two in 2014, and two in 2017-2018.

In advance to the planning of the first test series, loading methods in the past beam component tests were reviewed with probable effects of floor slabs. As a result, a special loading set-up was developed and used for the frame assembly specimens consisting of four columns and four beams with lengths of one span and two half spans in two directions. The four columns were loaded laterally and independently at mid-height of the upper story and supported at mid-height of the lower story with pin-fixed and pin-roller so that the axial elongation of beams and slab would not be constrained but would be free at one end of the two.

The two specimens in the first test series of 2010 were two-fifth scale three-dimensional reinforced concrete beam-yielding frame with floor slab consisting of four columns and two frames in both directions, which simulated medium-story of high-rise buildings from lower to higher mid-heights of columns using high-strength materials. The damage patterns as well as the lateral resistances of the frames in various inter-story drift ratios were investigated considering the contributions of the slab to the beam resistance. It was found from the test that the stress in the slab reinforcing bars were increasing almost uniformly through the whole slab width and was fully effective to the flexural strength of the beams at one percent story drift and more. The results of the 2010 tests and analysis have been reported elsewhere.

Three specimens were tested in 2013, one with slab, another without slab, and the third a with relatively shallow beams representing a medium-story of mid-high-rise building using normal-strength materials. The effects of slab could be identified directly by comparing the strengths of the specimens with and without slab. A connecting through detail for the slab lower chord rebars was also adopted to compare with a cut-off detail of slab lower chord rebars used in practice. At the inter-story drift of 1/75-1/50, the beam capacity in slab tension exceeded the calculated flexural strength assuming the full width of slab and all slab reinforcement. The flexural capacities at each beam ends of the inner beams and the outer beams were evaluated and compared with the calculation based on flexural theory assuming full width of slab. The 2013 test results and main findings are reported here in this paper.

The 2014 specimens represented an outer span at one end and the slab thickness was varied: one was normal slab and the other thick void slab in half scale to identify the effect of the rigidity of the transverse beams at the end span. The effective widths in case of relatively weak transverse beams were further studied in 2017 and 2018.

Keywords: floor slab, effective width, frame assembly test, axial elongation, earthquake loading
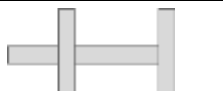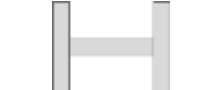
1. Introduction

Seismic performance of reinforced concrete buildings in Japan shall be verified through a standard design procedure in two phases by checking the serviceability in the first phase and the safety in the second phase in accordance with the Building Standard Law of Japan, pertinent regulations and design code of practice. The ultimate lateral load carrying capacity is checked against the demand which is equivalent to the response under a very rare event based on static pushover analysis taking inelastic deformation capacities and the collapse mechanism into account. An overall and ductile beam-yielding collapse mechanism is to be selected mostly for medium- to high-rise reinforced concrete buildings, where the effects of the floor slabs are significant in the evaluation of the beam ultimate flexural strengths. A series of static and seismic loading tests of reinforced concrete frame assemblies were planned and conducted in 2010, 2012, 2013, 2014 at Building Research Institute to identify the effects of slab as part of national research projects for review of the technical standards on seismic design practices in Japan. The research theme is succeeded also by another series in 2017 to 2018 at Tokyo Metropolitan University as listed in Table 1.

Three specimens in the first series of 2010 were two-fifth scale three-dimensional reinforced concrete beam-yielding frames with floor slab consisting of four columns and two frames in both directions. The high strength materials were used representing high-rise buildings. A special loading set-up was invented and used to simulate the boundary conditions of the medium-story frame so that the axial elongation of the beams would not be constrained by the reaction supports at the columns. One of the two specimens was repaired and tested again in 2012 to verify the seismic performance after repair. Three specimens tested in 2013 and two in 2014 using normal strength materials to represent medium-rise reinforced concrete frame buildings with different parameters. The damage patterns as well as the lateral resistances of the frames in various inter-story drift ratios were investigated considering the contributions of the slab to the beam resistance to reconsolidate the current design practice. Here are reported in this paper an outline and backgrounds of the test series including the test results in 2013, new findings from the serial tests and analyses, and design implications derived from the test series, such as effective slab widths for analytical modelling and evaluating ultimate strength of beams in seismic design in relation with drift responses.

Table 1 – A series of slab frame assembly tests from 2010 to 2018

Year	Assembly	Specimen	Prototype/ Materials	Parameter	Note
2010		No. 1 No. 2	High-rise High strength	Slab reinforcement ratio	Full width effective at 1/100
2012	Repaired after 1/30 loading	R (No. 2)	Repaired after 1/30 loading	Post EQ Repair	100% Strength, 60% Stiffness recovered
2013		S (No. 3) F (No.4) SB (No. 5)	Med-rise Normal strength	With slab Without slab Shallow beam	Comparison with/without slab Inner end＞Outer end
2014		SE (No. 6) BE (No. 7)	Mid-rise Normal strength	End span Axial loading	Continuous beam＞End beam
2017		2017 (No. 9)	Low-rise Normal strength	Beam rigidity (low)	Narrow slab width due to flexible transverse beam
2018		2018 (No. 9)	Low-rise Normal strength	Beam rigidity (high)	Wide slab width owing to rigid transverse beam

2

2. Effective slab widths in design and tests

2.1 Effective slab width in design

The effective slab width in the elastic analysis for the first phase design is prescribed in the AIJ guidelines [1] as approximately one tenth of the beam longitudinal length, as shown in Fig. 1(a). The effective slab width is evaluated mainly to derive the equivalent stiffness of T-beam section in the frame model for linear analysis, while the effects of slab reinforcing bars on the flexural strength is normally neglected during the first phase design. On the other hand, the effective slab width is taken as a constant length of 1.0 meter on each side of the beam for the pushover analysis in the second phase design [2], as shown in Fig. 1(b). The slab reinforcing bars within the effective width may be taken into account for the evaluation of the ultimate flexural strengths of the beams. However, only the slab reinforcing bars in the upper chord have been counted in practice when the slab is in tension neglecting the slab bars in the lower chord because the anchorage lengths of the lower chord bars have been regarded as insufficient to develop the full tensile strength in accordance with the normal practice of construction details.

The standard assumptions for the effective slab width described as above have been used commonly in analytical models and strength evaluation, not only for static analyses of low and medium rise buildings in the two design phases, but also for time-history response analyses of high-rise buildings.

Effective slab width
ba=0.1*l* (a/l>0.5), *l*:beam length

Upper slab rebars
In the range of 1.0m width

(a) Effective slab width for the first phase design　　(b) Effective slab width for the second phase design
Fig. 1 – Effective slab width for beams in the Japanese seismic design code of practice

The assumptions above on the effective slab widths, especially those for the second phase evaluation, seemed to be conservative because most of past tests on beams with slab or one column sub-assemblage tests performed in 1980s or early 1990s showed much higher effects on the beam flexural strengths at the ultimate deformations. However, the effective widths observed in the tests were gradually increasing with the inelastic drift amplitudes to attain wider widths so that the design practices have still been maintained as above. On the other hand, the effectiveness of slabs has also been examined through recent laboratory tests on full-scale building structures under static, pseudo-dynamic, or dynamic loading, where the measured overall capacities were close to those calculated by assuming the full span slab width in most cases. It should be noted that the conservative evaluation on the effective slab widths may not always be safe from the viewpoint of ensuring flexural failure mode and/or beam yielding mechanism in the structure. Therefore, it is important to take in account a probable effective slab width in the seismic design calculations, especially, in the assurance design to estimate beam shear and column actions in the overall beam yielding mechanism. Not only the ultimate strength but also the hysteretic relations of the beam-slab component could be different from the current models for time-history response analysis. Therefore, the seismic performance of the beams with floor slabs need be further verified through realistic tests and analyses.

2.2 New method of testing beam-column assembly with slab

Based on the review of past test research, a new loading method of testing frame assembly with slab was planned and applied to validate the effectiveness of the floor slab on the beam in the current design evaluation including frame analyses. In the first 2010 project, a thirty-story building was selected as a proto-type design for the test specimens. The two-fifth scale specimens were designed and constructed, as shown in Fig. 2(a) and in the attached photo, representing part of interior frames with floor slab in a middle story of the proto-type building. Four columns from lower mid-height to upper mid-height and the beams with floor slab of one span and two half spans in each direction were extracted.

3
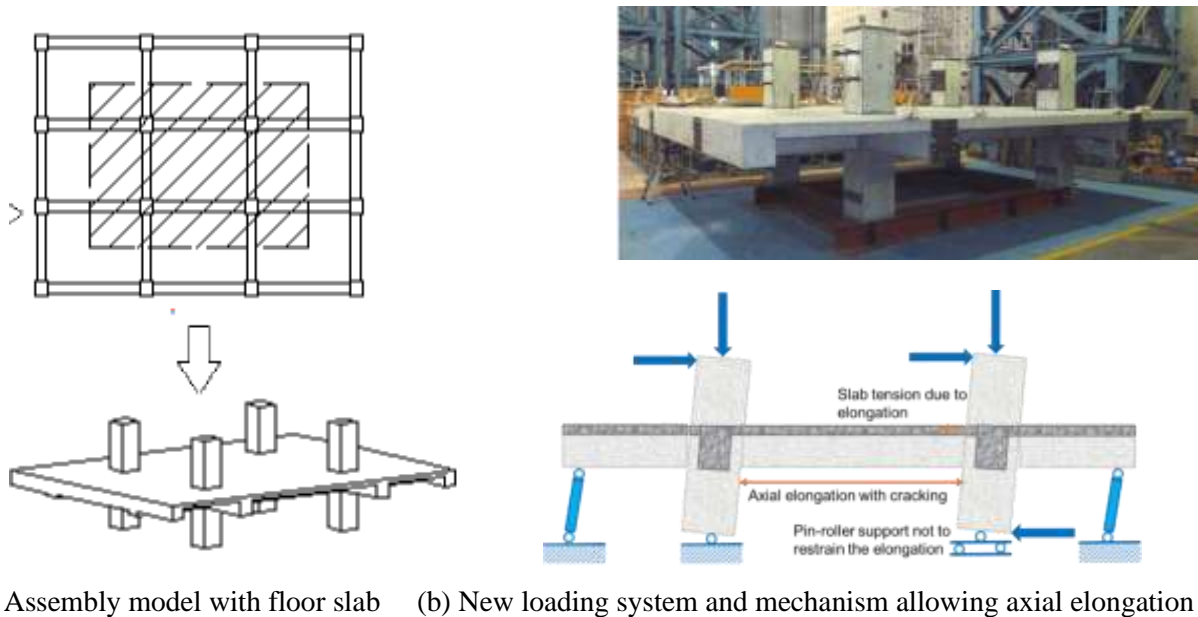
(a) Assembly model with floor slab   (b) New loading system and mechanism allowing axial elongation

Fig. 2 – New loading method and slab assembly specimen representing moment-resisting frame to expected mechanism

A series of three-dimensional frame tests were carried out under static cyclic lateral loading to investigate the hysteretic behavior with the contribution of the slab in the beam-yielding frames from 2010 to 2014 [3, 4, 5, 6]. A special loading set-up was invented to be used for the frame assembly in the test series. The four columns were loaded laterally and independently at mid-height of upper story and supported at mid-height of lower story with pin-fixed and pin-roller so that axial elongation of the beams and the slab would not be constrained by the lateral forces, as shown in Fig. 2(b). Also, special consideration was made with respect to the boundary conditions at the mid-height columns so that the axial elongations in the beams were not constrained. Beam resistance including the slab might be different at interior and exterior beams. It is expected at the interior beams that axial elongation would occur due to cracking, as shown in the figure, so that the slab reinforcement could be effective simultaneously with the beam reinforcement over the full width of slab as the reaction of the beam compressive force. On the other hand, the effectiveness of the slab at the exterior beam would occur at larger deformation due to the boundary condition at the end.

3. Test methods

3.1 Frame assembly specimen with/without slab tested in 2013

The second test series in 2013 are reported here which compared frame assemblies with and without slab. The specimens were reduced by two-fifth scale following the slab assembly specimens of the first 2010 tests. Specimen F without slab and Specimen S with slab were constructed and tested. The common geometric sizes of the specimen are shown in Fig. 3. The height of the specimen was 2010mm with 1085mm upper columns and 925mm lower columns measured from the center of the beam, though the story height was 1360mm between the lower to the upper mid-height for loading. In the longitudinal direction, the center-to-center middle span length was 3200mm, while the center-to-end half-span was 1600mm. In the transverse direction, the center-to-center middle span was 2500mm, while the center-to-end half-span was 1250mm. The column sectional dimensions were 400mm by 400mm. The width of the main beams was 300mm and a depth of 360mm in two directions. The transverse beams of 220mm by 290mm were placed for loading at the two ends assuming the inflection point at the middle of the continuous beam span in both directions. The slab thickness was 100mm.
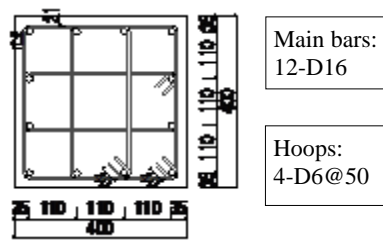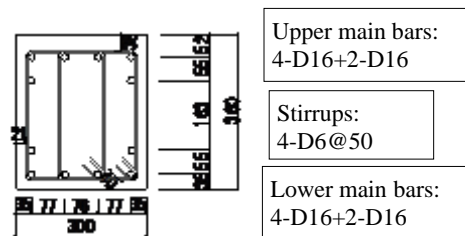
2b-0077
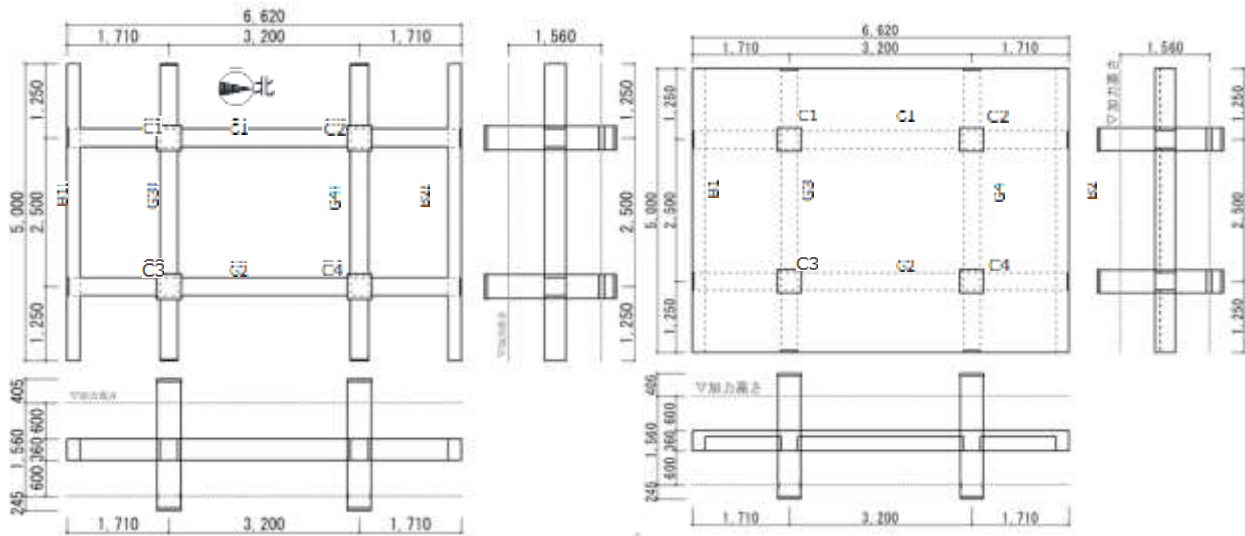
(a) Specimen F without slab　　　　　　(b) Specimen S with slab

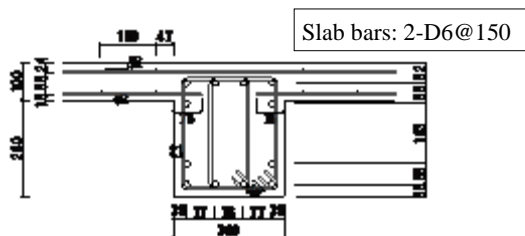Fig. 3 - Geometry of Specimen F and Specimen S

　　　The reinforcement details are shown in Figs. 4(a) - (d). The main bars of the columns were 12-D16 (SD390) with the gross sectional ratio of 1.51% and the column hoops were 4-D6@50 (SD295). The beams had 6-D16 at the top and 6-D16 at the bottom (SD390) as main bars with the gross sectional ration of 2.23%, both arranged in two layers as shown in the figure. The stirrups in the beams were 4-D6@50 (SD295). The main bars of the columns and beams were welded to the steel plates at the ends. The concrete was cast in three stages, consisting of: 1) lower columns and joints, 2) beams and slabs, and 3) upper columns.
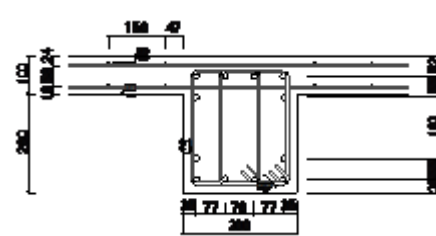

Main bars: 12-D16

Hoops: 4-D6@50

Upper main bars: 4-D16+2-D16

Stirrups: 4-D6@50

Lower main bars: 4-D16+2-D16

(a) Column section of Specimen F and S　　　(b) Beam section of Specimen F

Slab bars: 2-D6@150

Cut-off detail of lower slab rebars in common use　　　Connecting through detail of lower slab rebars

(c) South transverse beam section of Specimen S　　(d) North transverse beam section of Specimen S

Fig. 4 – Reinforcement details in columns, beams and slabs of the specimens in 2013 tests

　　　As shown in Figs. 4(c) and (d), deformed bars with the diameter of 6mm (D6) and the nominal yield strength of 295MPa (SD295) were placed at the spacing of 150mm at the upper and lower chords (2-D6@150) in both directions for the floor slab of Specimens S. Two types of anchorage details for the lower slab reinforcement were compared: one at south transverse beam in conventional detail of practice in Japan, as

5

shown in Fig. 4(c), a cut-off detail with the anchorage length of 75mm corresponding to 150mm in full scale and common use, while the other at north transverse beam, as shown in Fig. 4(d), a connecting through detail with sufficient anchorage length. The anchorage length in the cut-off detail is insufficient for full anchorage length for pull out force, so that the lower chord slab rebars is not included in practical calculation of ultimate flexural strength of beams in taking into account the effect of slab reinforcement.

Concrete cylinder tests were conducted at the date of testing. Normal strength materials were used for both steel and concrete in the specimen to represent the design of proto-type medium-rise buildings. The actual material properties from the tests are shown in Table 2 and Table 3.

Table 2 – Material properties of concrete

Specimen	Part of the specimen	Nominal Strength N/mm²	Compression strength N/mm²	Tensile strength N/mm²	Elastic Modulus N/mm²
Specimen S	Lower column	Fc30	40.8	2.81	28900
	Beam and slab	Fc30	45.6	3.42	32400
	Upper column	Fc30	42.1	3.51	34400
Specimen F	Lower column	Fc30	44.2	3.15	28800
	Beam and slab	Fc30	48.5	3.09	29900
	Upper column	Fc30	39.6	3.06	27700

Table 3 – Material properties of reinforcing steel bars

Nominal diameter	Nominal strength	Yield strength N/mm²	Yield strain (x10⁻⁶)	Elastic Modulus N/mm²	Max. strength N/mm²
D16	SD390	455	2414	188000	649
D6	SD295	448	2414	185000	523

The loading setup is illustrated in Fig. 5(a). The two columns on the south side were supported with pin ends assuming the inflection points as mid-height of lower columns, while the two columns on the north side were supported with pin-roller ends, so that the axial deformations would not be restrained by the axial forces caused by the beam and slab elongation increasing with the inelastic deformations. The transverse beams at both ends of the outside half-spans were supported in the vertical direction with the pin-end jacks and the load cells simulating the inflection points at the mid-span. H-shaped steel beams of 200mm by 200mm size were appended to increase the stiffness and strength at the top of both end beams additionally. A constant axial load of 990kN was applied at each top of the four columns using vertical actuators with pin-connected to the column at the bottom end and roller support at the top end of the actuators, which could move freely by four 2-D roller supports attached to two big steel beams on the top. Seismic loads were applied to the tops of the columns using four jacks and to the pin roller supports at north side were also loaded by two jacks. The pin supports were fixed to the concrete base.

The details of the pin and pin roller supports at the column bases are shown in Fig. 5(b). The steel footing of pin support was fixed on the foundation, while the steel footing of pin roller support was just placed on a smooth plastic plate so that transversal movement was allowed. Steel rods of 75mm diameter welded on the steel footing were attached to the column faces to apply horizontal force or reactions. Two smooth steel curve face plates with a radius of 750mm were manufactured. One was connected to the column bottom, and another one was just put under it and could move freely with the rotation of column. An overview of the loading setup at large structural laboratory, Building Research Institute, Tsukuba is shown in Photo 1.

To simulate vertical loads of medium-rise buildings, an axial force of 990kN was applied to each column and kept constant by the four vertical actuators. The averaged compressive stress in the column section was 0.20 times the nominal concrete strength (Fc30) corresponding to that of columns carrying ten stories above. Then static lateral cyclic forces were applied with six lateral oil jacks. The south jacks and the north jacks were operated independently. The north jacks of upper and lower stories were operated to keep the same level but in the opposite directions by the common oil pressure, while the story drift angles of the south columns were synchronized to those of the north columns controlled manually through the instantaneous feedback data from

6

the lateral displacement gauges at the upper and lower loading level of each column. The increasing drift amplitudes of cyclic loading were shown in Fig. 6. The cyclic loadings were reversed at the peak drift angles of R=$\pm 1/400, \pm 1/300, \pm 1/200, \pm 1/150, \pm 1/100, \pm 1/75, \pm 1/50, \pm 1/37.5, +1/25$ (rad.), two cycles for each peak but one cycle of $\pm 1/300$ and positive half of $+1/25$.

(a1) Plan

(b1) Pin support   (b2) Pin roller support

(b) Details of pin support and pin-roller support

(a2) Elevation
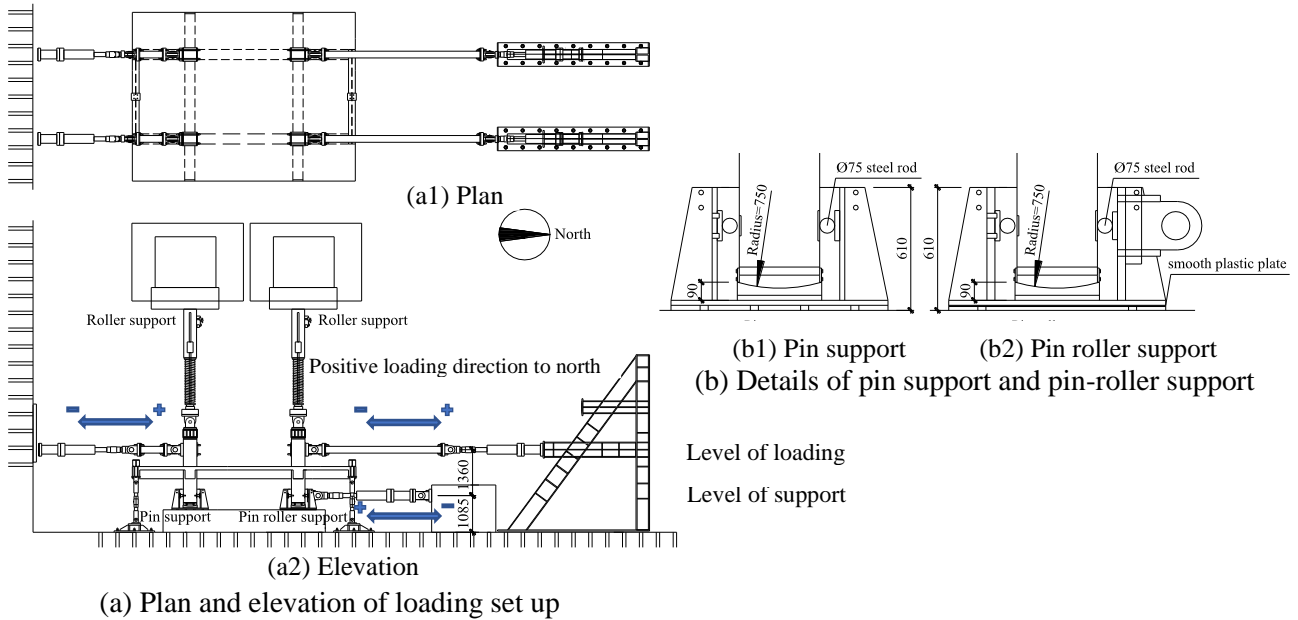
(a) Plan and elevation of loading set up
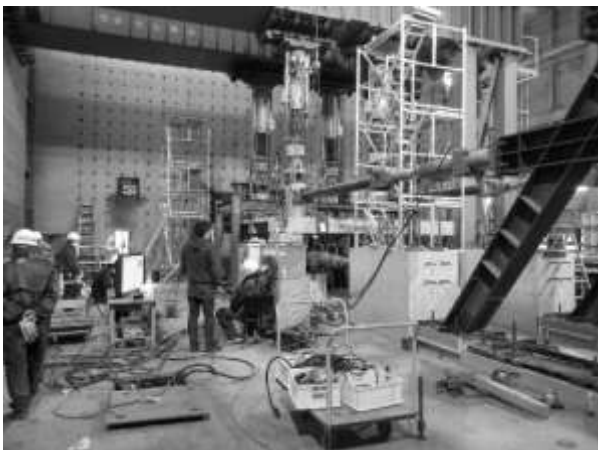
Fig. 5 – Loading methods

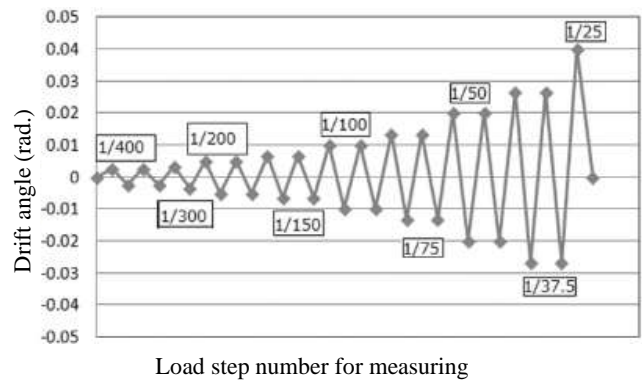Photo 1 – Loading Setup, Building Research Institute

Fig. 6 – History of loading in story drift ratio

Local deformations and strains in reinforcement were measured by displacement gauges and wire strain gauges as dense as possible. Lateral displacements of each column were measured at the top and the bottom of loading levels, also at the floor level, from which lateral deflection of columns and overall elongations were derived. Local axial deformations, or elongations, rotations were measured on the surfaces of slab and beams and also on the column side faces using displacement gauges and sliding pipes with universal joints at each end. Relatively dense measurement was planned at the slab surface at the critical sections to drive slab effects by the distribution of axial elongations at the sections. The strains were measured on the reinforcement in the beam and the slab not only at the critical sections but also at points away from the critical sections.

7

## 4. Test results on frame assemblies with/without slab

4.1 Observed cracks

The crack patterns observed after loading cycles with the peak drift of 1/50 rad. in the east beam sides and top surfaces of Specimen F and Specimen S are shown in Fig. 7(a) and Fig. 7(b) respectively. Cracks shown with red lines occurred in positive direction of loading and with blue lines in negative. Initial cracks observed in the slab surface of Specimen S immediately penetrated to the whole width of slab and also to the bottom. The cracks on the inner span were perpendicular to the longitudinal beams or parallel to the transverse beams, while the cracks on the outer half-spans were inclined, as shown in the figures. These might be because of the boundary conditions and associated resistance mechanisms, which were different between the inner and outer spans. The cracking of the column was minor owing to high axial load and higher flexural strength. These differences in crack patterns were also observed in the first test series in 2010. As for the cracks at the side faces, generally vertically perpendicular to beam axis in Specimen F, while a bit inclined in Specimen S, probably due to the higher shear/moment in the slab tensile direction.
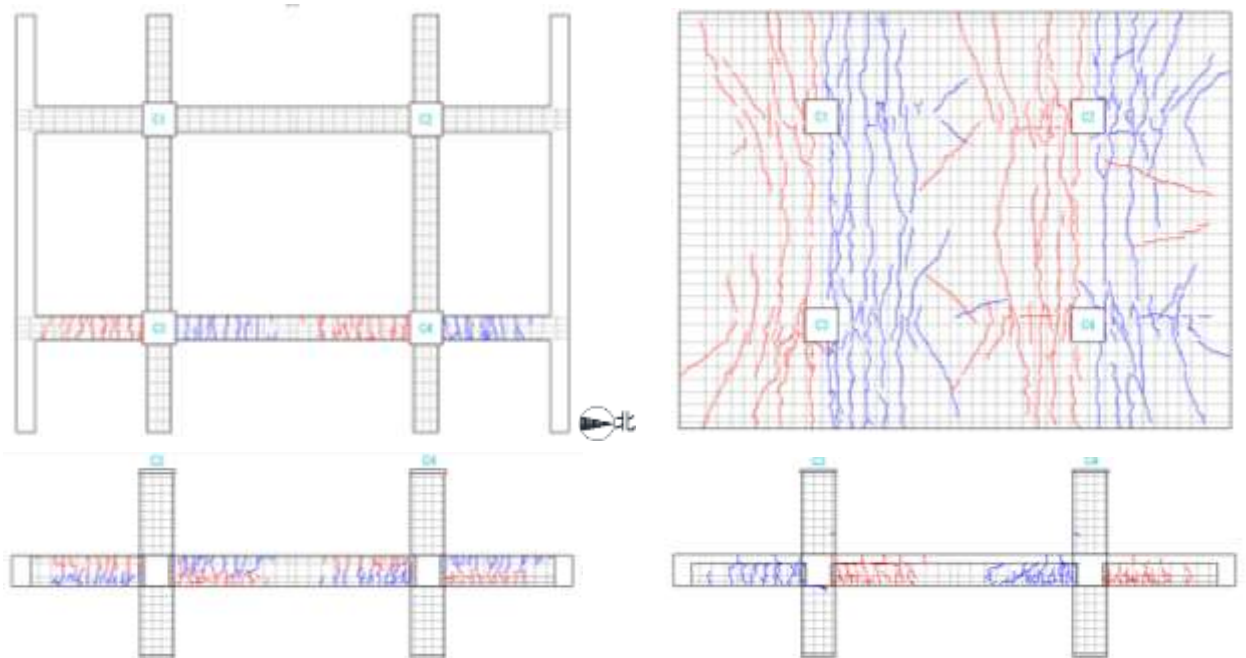
(a) Cracks of Specimen F　　　　　　　　　(b) Cracks of Specimen S

Fig. 7 – Cracks observed at 1/50(rad) peak of Specimen F and Specimen S
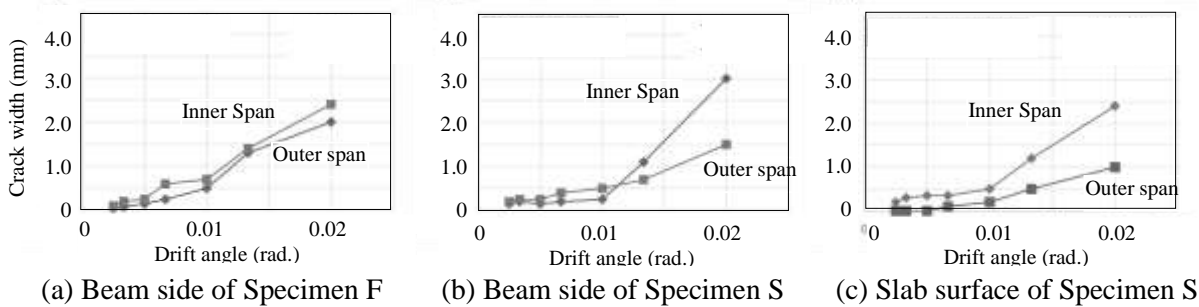
(a) Beam side of Specimen F　　(b) Beam side of Specimen S　　(c) Slab surface of Specimen S

Fig. 8 – Maximum crack widths measured at drift peaks of Specimen F and Specimen S

Maximum crack widths measured at each peak drift of loading cycles are shown in Fig. 8 with relations to the story drift. The maximum values of the crack widths are distinguished between at the outer span and at

8

the inner span of the longitudinal beams and the slabs. The crack widths on the slab faces and on the beam sides in Specimen S are generally wider at the inner span beams than those at the cantilever outer beams, while cracks of Specimen F are similar in widths at the inner span beams and at the outer span beams.

4.2 Measured strains in slab reinforcement

Strains in the slab reinforcement at the critical sections of the inner span beam of Specimen S were measured along the slab width in the transverse direction at the critical section 40mm apart from the column face line. Distributions of the strains measured in the upper slab rebars along the slab width of the inner span beams are shown in Fig. 9. The strain corresponding to yielding strains is shown with dotted lines. The slab strains started to attain the yielding level prior to drift of 1/200rad in the vicinity of longitudinal beam. The strains are smaller but close to the yielding level uniformly in the wide region to the transverse direction.

The stains were measured also in the lower chord slab rebars. As shown in relation to the overall drift angle in Fig. 10, the strains are compared for the different anchorage details, one with conventional the cut-off detail shown in Fig. 4(c) and the other with the connecting through detail in Fig. 4(d). Although it has been neglected in design calculation due to an insufficient anchorage length of 10d (150mm in full-scale) by the detail of practice, it may be concluded that most of the slab reinforcement attained around 1500micro level of strains, which is around 75% of yielding stains beyond a story drift of 1/75 as measured in the upper rebars. The averaged stains in the upper rebars are increasing more while those in the lower rebars are not but limited after 1/75, which might be due to pull out at the anchorage. However, it may be concluded that the lower chord rebars in the conventional detail would also be effective to carry some amount of tensile forces along full width of slab. In case an enough anchorage length is adopted for the lower chord rebars such as connecting through, it is expected that these would also be fully effective up to the yield level.
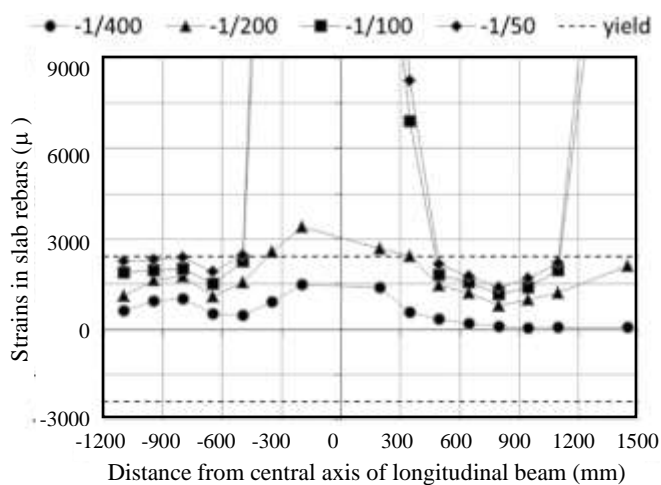

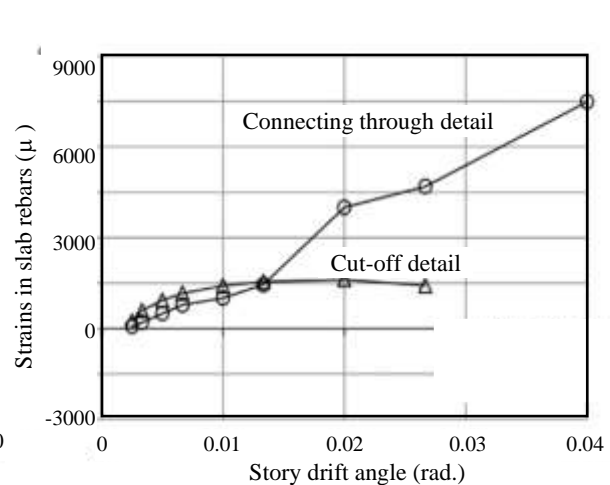Fig. 9 – Strain distributions along the slab width   Fig. – 10 Strains in lower chord slab rebars

4.3 Overall hysteresis and calculated strengths

The overall hysteretic responses for story shear force versus story drift angles of Specimen F and Specimen S are shown in Fig. 11 with black line and red line respectively. The story shear force is directly derived as the sum of the lateral shear forces applied at the loading level of the column tops. The story drift angles are derived from the horizontal displacements measured at the loading level at the column tops relative to the horizontal displacements measured at the pin and pin-roller supporting level at the column bases.

The main beam rebars of Specimen F, an open frame assembly without slab, started to yield at around the story drift of 1/150 rad at the first end row and 1/100 at the second mid row. The resistance at the peaks was increasing and maintained stably up to the ultimate loading level with the drift of 1/25 rad. The main beam rebars of Specimen S, a frame assembly with slab, started to yield at around the story drift of 1/100 rad at the first end row. The resistance at the peaks was increasing and maintained also stably up to the ultimate loading

9

level with the drift of 1/25 rad. A slight pinching was observed in the hysteresis loops of Specimen S, which is general characteristics due to asymmetric strengths in positive and negative bending moment with the effect of slab.

Calculated strengths for Specimen S in terms of the overall story shear force are also shown in Fig. 11 with two lines, both by assuming full slab width based on flexural theory: one with red dashed-two dotted lines by assuming all slab rebars in the full slab width to be effective and the other with red dashed-dotted lines by assuming only upper chord slab rebars for the cut-off detail end in south transverse beam. Calculated strength for Specimen F without slab is shown with black dashed-dotted line in the figure.

As compared with the measured resistance of Specimen F, the resistance of Specimen S is not very much higher up to the drift of 1/100 around yielding deformation. The differences in the resistances are obvious beyond the yielding level, which become close to the differences in above calculation after the drift of 1/50. The overall strengths of Specimen S exceeded not only the second full width calculation but also even the first full width calculation with all slab rebars at the drift of 1/50rad. The deformation level of fully effective slab was larger than those by 2010 test at around 1/100-1/75rad, which might be due to normal strength or not very high strength of concrete in the2013 test specimens, resulting in smaller effective depth in slab tensile bending. The measured overall strength of Specimen F exceeded the calculated strength at 1/100 rad. and increasing still more at the larger drift level. By comparing the resistances of the two specimens, it may be concluded that the additional strengths by the effect of slab is close to or slightly smaller than the difference in calculation assuming all slab rebars including lower chord along the full width.
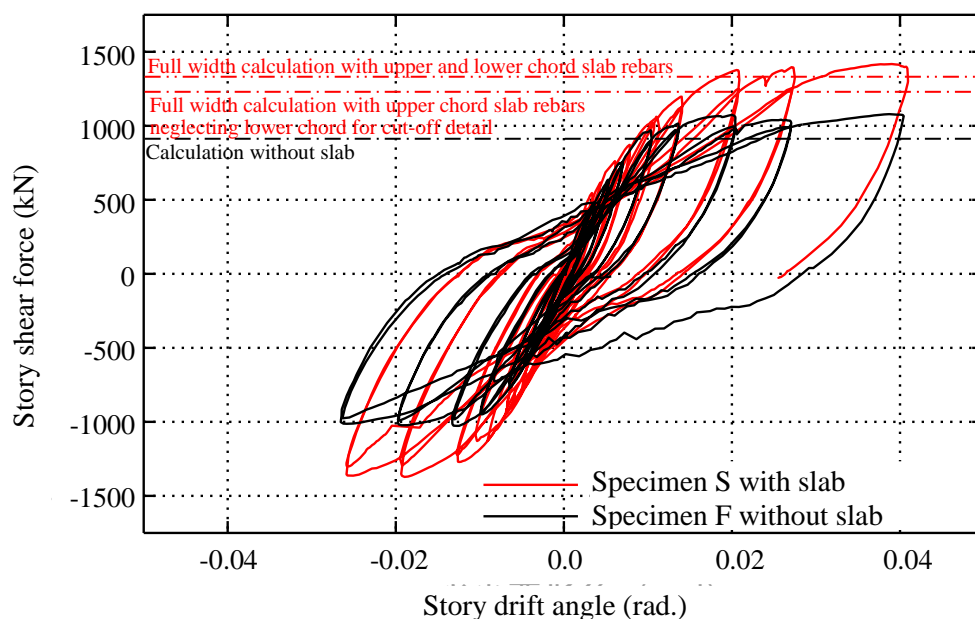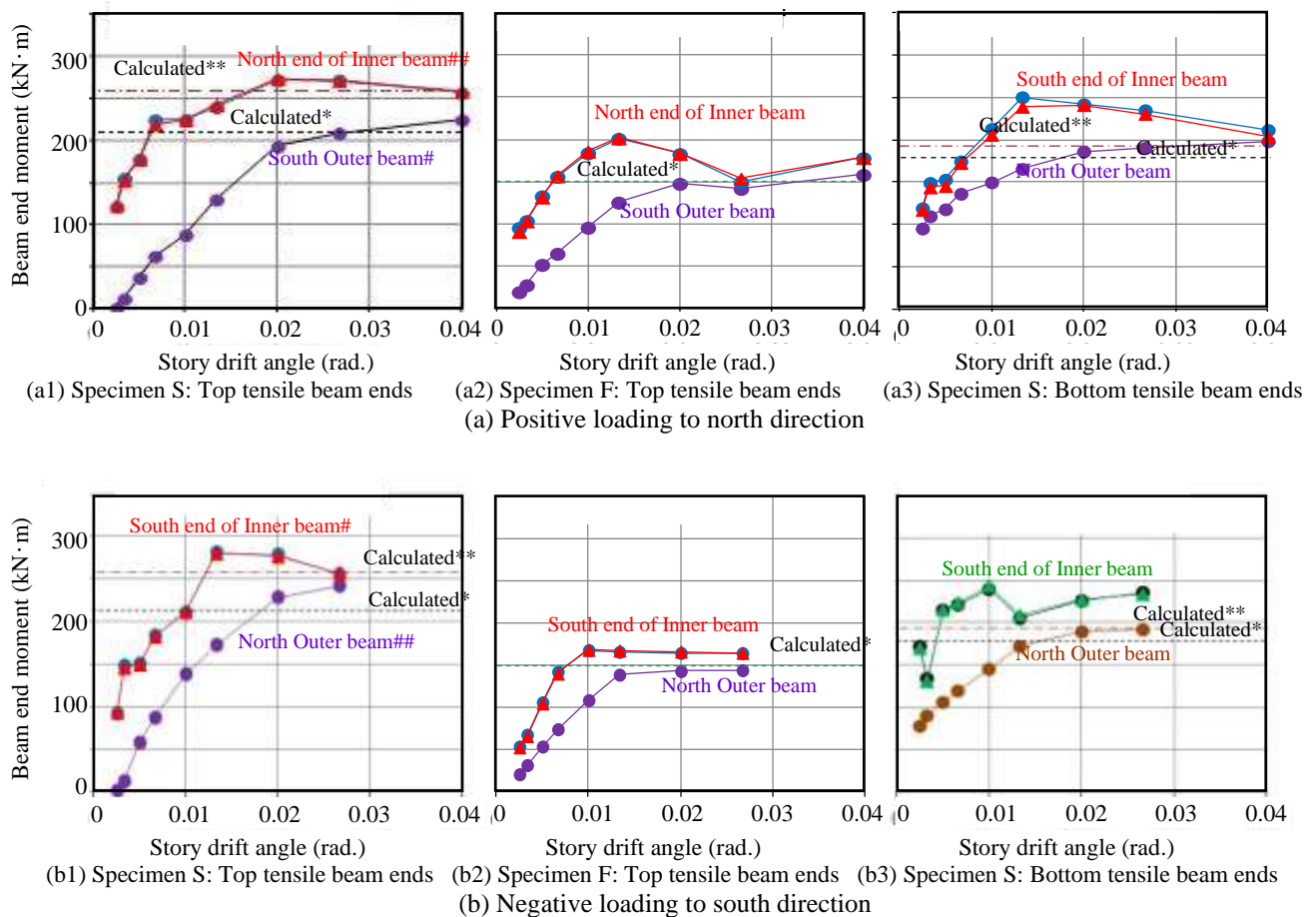

Fig. 11 – Hysteresis relations of overall story shear and story drift

From the lateral loads measured independently at the column tops and bottoms and also from the vertical reaction forces measured in the supporting rods at both ends of the specimen, beam end moment at each critical section can be identified as shown in Fig. 12 for each loading peak in positive and negative direction. The beam end moments are shown distinctively for top or bottom tensile bending, inner or outer beam, positive or negative loading direction and specimen S or F. The column forces are independent so that the end moment can be evaluated at each of two inner beam ends, which was almost identical actually, while the vertical reaction rod is one at each end and the measured force is the sum of two cantilever beams so that moment of one beam as averaged for the two is shown in the figure, also with the calculated flexural strength of beam section taking into account the effect of slab in both direction of bending for Specimen S by assuming the lower chord slab rebars to be effective or not. The outer beam moment is relatively smaller but increased gradually approaching to the inner beam strength finally.

10

As shown in Figs. 12 (a1) and (b1), the bending moments of the inner beam are generally larger than those of the outer beam. The inner beam moment attained the calculated strength at around 1/75 assuming both upper and lower chord slab rebars to be effective along the full width both connecting through detail (a1) at north and also cut-off detail (b1) at south. The ultimate strength of the outer beam south with the cut-off detail (a1) in positive loading is smaller and slightly exceeding the calculation without lower chord slab bars. Even in case of Specimen F without slab shown in Figs. 12 (a2) and (b2), the inner beam moment is generally larger than the outer beam moment, especially around smaller drift levels. This is also the case with the bottom tensile moments of the beams with slab in Specimen S as shown in Figs. 12 (a3) and (b3), which exceed the calculated strength especially at the inner beam ends. It might probably be due to insufficient restraining rigidity by the rod at the cantilever beam end as discussed elsewhere [6] though needs be investigated further.

(a1) Specimen S: Top tensile beam ends   (a2) Specimen F: Top tensile beam ends   (a3) Specimen S: Bottom tensile beam ends
(a) Positive loading to north direction

(b1) Specimen S: Top tensile beam ends   (b2) Specimen F: Top tensile beam ends   (b3) Specimen S: Bottom tensile beam ends
(b) Negative loading to south direction

Notes:
Calculated**: Flexural strength calculated by assuming full width of slab and with both upper and lower chord slab rebars
Calculated*:   Flexural strength calculated by assuming full width of slab and with only upper chord slab rebars
South beam#: Cut-off details of lower chord slab rebars into south transverse beam
North beam##: Connecting details of lower chord slab rebars into north transverse beam

Fig. 12 Beam moment resistance in upper side tension at negative loading to south

5. Conclusions

A series of frame assembly tests were conducted to investigate the effective slab width when calculating the ultimate strengths of beams in reinforced concrete buildings from 2010 to 2018. Here the results from the 2013 test where two specimens with/without slab are reported and discussed in detail, from which the following conclusions may be drawn:

11

(1) The observed crack patterns and measured strains in slab reinforcement for Specimen S with slab indicated that the slab would be effective widely along the full span width. The measured overall strengths of Specimen S attained the calculated strength by assuming the full effective slab width and all of the reinforcement based on flexural theory at the story drift of 1/50rad, which was larger than those by the 2010 test using high strength concrete.

(2) As compared with Specimen F, the resistance of Specimen S was not very much higher up to around yielding drift of 1/100 but exceeded gradually and attained the full-width calculation around the drift of 1/50. The strength of Specimen F attained the calculated strength at 1/100 rad. The additional strengths by the effect of slab was close to or slightly smaller than the calculated difference assuming all slab rebars in full width.

(3) The flexural strength of the inner beams attained the full-width calculated strength at the story drift of 1/100rad, while the outer beams attained the calculated strength at much larger deformation exceeding 1/50rad. The bending moments of the inner beam are generally larger than those of the outer beams especially in the smaller drift levels. The inner beam moments are generally larger also in case of Specimen F without slab. One of the reasons is estimated to be insufficient restraining force at the outer beam ends, which needs be investigated further in detail.

(4) The anchorage details of the lower chord slab rebars to the transverse beam were varied and compared in two ways: one with 75mm development length (corresponding to 150mm in full scale) in accordance with the conventional design practice, and the other with fully continuous development in connecting through to the opposite beam face. In spite of insufficient length for perfect anchorage in the conventional detail, the strains in the slab rebars indicated the averaged resistance close to yielding was kept effective after the drift of 1/75. The connecting through detail was more effective and the measured strains were increasing up to the final stage of loading much exceeding the yielding strain.

6. Acknowledgments

7. References

[1] Architectural Institute of Japan (2009): *AIJ Standard for Structural Calculation of Reinforced Concrete Structures (in Japanese)*, (Article 8: Basics of structural analysis), AIJ, 63-64.

[2] Building Center of Japan (2007): *Guidelines for Structural Standard Requirements on Buildings (in Japanese)*, BCJ, 620-663.

[3] Toshimi Kabeyasawa, Toshikazu Kabeyasawa, Deng Xuan, Hiroshi Fukuyama (2015): Frame test on effects of slab to beam strength in reinforced concrete buildings (in Japanese), *Journal of Structural Engineering*, Architectural Institute of Japan, Vol.61B, 103-110.

[4] Toshimi Kabeyasawa, Toshikazu Kabeyasawa, Hiroshi Fukuyama (2017): Effects of Floor Slabs on the Flexural Strengthof Beams in Reinforced Concrete Buildings, *Bulletin of The New Zealand Society for Earthquake Engineering*, 50, 4, 517–526.

[5] Toshimi Kabeyasawa, Toshikazu Kabeyasawa (2017): Effective Slab Width For Evaluating Ultimate Seismic Capacities of Reinforced Concrete Buildings, *Proceedings of the 4th Congr`es International de G´eotechnique - Ouvrages -Structures* , ISBN 978-981-10-6712-9, 300–309.

[6] Toshimi Kabeyasawa, Toshikazu Kabeyasawa: Effective Slab Width for Evaluating Seismic Performance of Reinforced Concrete Structures, *SEFC 2015 Proceedings*, Structural Engineering Frontier Conference, Yokohama, Japan, March 18-19, Tokyo Institute of Technology, 1–22, 2015.